International Journal of GEOMATE, Feb., 2021, Vol.20, Issue 78, pp. 36-43
ISSN: 2186-2982 (P), 2186-2990 (O), Japan, DOI: https://doi.org/10.21660/2021.78.95188
Geotechnique, Construction Materials, and Environment

TWO-DIMENSIONAL PHYSICAL MODELING OF MULTI CHAMBER SKIRT BREAKWATER (MCSB)

Azis Ali Wibowo[1], Ricky Lukman Tawekal[1], *Harman Ajiwibowo[1], and Andojo Wurjanto[1]

[1]Faculty of Civil and Environmental Engineering, Institut Teknologi Bandung, Indonesia

*Corresponding Author, Received: 06 Sep. 2020, Revised: 08 Nov. 2020, Accepted: 27 Dec. 2020

ABSTRACT: Multi-Chamber Skirt Breakwater (MCSB) is a skirt-type breakwater consisting of piles at the lower part, and two chambers skirt with porosity in the upper part of the structure. The additional number of chambers with variations of chambers gap length is expected to increase the breakwater's effectiveness. Physical modeling is conducted to examine the transmission coefficient (C_T) and the reflection coefficient (C_R). The relationship between environmental and structure independent variables with the transmission and reflection coefficient is investigated. The physical modeling concluded that the structure's transmission coefficient in the deep water is less than 0.31, while the intermediate-depth water condition is 0.31-0.72. The reflection coefficient is 0.36-0.51 for deep water and less than 0.5 for the intermediate depth water condition. It is concluded that MCSB is effective in intermediate-depth and deep water conditions where the range of the depth parameter (kh) is between 2.5 to 3.1.

Keywords: Multi-chamber skirt breakwater, Transmission coefficient, Reflection coefficient, Intermediate depth water, Deepwater.

1. INTRODUCTION

The construction of gravity-type breakwaters such as the rubble mound breakwaters in intermediate-depth and deep waters can be costly due to the high volume of rubble materials [1]. In such a case, the skirt-type pile breakwaters can replace the gravity-type for the less expensive and relatively less complicated construction method. In this study, a Multi-Chamber Skirt Breakwater (MCSB) structure is investigated.

The research aims to examine the effectiveness of the MCSB, which is presented by the transmission coefficient (C_T) dan the reflection coefficient (C_R) relationship with the environment and structure variables in the intermediate depth water and deepwater region. The intermediate-depth is in the region of $\pi/10<kh<\pi$, and the deepwater is in the region of $kh>\pi$ [2]. The physical modeling is carried out in the Ocean Engineering Laboratory at Bandung Institute of Technology, Indonesia.

Suh et al. [3] observed the effectiveness of a curtain-wall-pile breakwater using physical and analytical models. The model consists of a vertical wall and piles. The research is conducted in intermediate depth to the deep water condition. The analytical model is carried out using the velocity potential theory applying the monochromatic waves. The kinematic and dynamic boundary conditions are applied within the domain. The research concludes that the curtain-wall-pile breakwater produces larger transmitted and smaller reflected waves than the pile-supported vertical wall breakwater.

Koraim [4] investigated slotted breakwater's behavior, which consists of a vertical slot in one row using regular waves condition. The research observed the hydrodynamic characteristics of the breakwater using an analytic and experimental solution. The structure's effectiveness is represented by the value of the wave reflection and transmission, energy loss, and hydrodynamic forces on the structure for the various values of waves and structural parameters. The reduction of the incoming wave energy is found to be 20-50%.

Wurjanto et al. [5] observed the effect of two chambers perforated breakwater in shallow water conditions. The research studied the effectiveness of the breakwater chamber numbers in terms of the transmission coefficient. It is found that the perforated skirt breakwater with three chambers is more effective than breakwater with two chambers. The chamber's width also influences the effectiveness of breakwater, and it was found that the transmission coefficient increases while the width of the chamber decreases and decreases as the skirt's draft increases.

The study of energy dissipation on the skirt-type breakwater with a single chamber was conducted by Laju et al. [6]. The model consists of piles at the lower part and skirt barriers at the upper part. The eigenfunction expansion of the velocity potentials was applied at the front, middle, and rear skirt barrier. The water depth regime is set in the intermediate depth water region ($1.0 < kh < 2.6$). It was found that the chamber width has to be between 0.3 to 0.5L (L is the wavelength) for a maximum wave energy dissipation rate of up to 50%.

Suh et al. [7] investigated modified curtain-wall pile breakwater [1] using a circular pile, formulated a mathematical model, and validated it with a physical experiment. The research concluded that the reflection coefficient increases, and the transmission coefficient decreases as the gaps of the pile decreases.

Ajiwibowo [8] conducted three-dimensional physical models of Perforated Skirt Breakwater (PSB) to examine the structure's effectiveness through the value of the transmission coefficient. The research concludes that the structure can dampen the waves by up to 50% for a short wave period.

Ajiwibowo [9] examined the effectiveness of Single Curtain Pile Foundation Breakwater (SCPFB) by using the transmission coefficient (C_T) parameter in intermediate depth water. The experiment concludes that The SCPFB is almost 90% effective when applied with the curtain extended to half of the water depth and suggested continuing the research in the range of $kh>\pi$.

Ajiwibowo [10] conducted 2-D physical modeling to evaluate the effectiveness of Perforated Skirt Breakwater (PSB) by the value of the transmission coefficient (C_T). The investigation concludes that PSB effectively dampens the wave energy 30-70% for short wave.

2. SCALING AND DIMENSIONAL ANALYSIS

2.1 Scaling

The Froude similarity principle is used to formulate the scaling as written in Eqs. (1) and (2).

$$(\boldsymbol{F_r})_{\boldsymbol{prototype}} = (\boldsymbol{F_r})_{\boldsymbol{model}} \quad (1)$$

$$\boldsymbol{F_r} = \frac{\boldsymbol{v}}{\sqrt{\boldsymbol{gL}}} \quad (2)$$

where
F_r = Froude Number
v = flow velocity
g = gravitational acceleration
L = length dimension

From a consideration of laboratory capacity, a scale of 1:12 is determined. Tables 1 and 2 show the structure and environment variables of the modeling, respectively.

2.2 Dimensional Analysis

The dimensional analysis is conducted to produce the dimensionless parameters that will be varied during the modeling. The dimensional analysis is carried out using the Buckingham π method [11]. The dimensionless variables are shown in Eqs. (3) and (4).

$$C_T = \Pi\left(kh,\ \frac{H_I}{L}, \frac{s}{h}, p, \frac{L_c}{h}\right) \quad (3)$$

$$C_R = \Pi\left(kh,\ \frac{H_I}{L}, \frac{s}{h}, p, \frac{L_c}{h}\right) \quad (4)$$

where
C_T = transmission coefficient
C_R = reflection coefficient
$k = \frac{2\pi}{L}$ = wave number
L = wavelength
L_c = length of chamber
s = draft of the skirt
p = skirt porosity

The dimensionless variables studied are the correlation between the transmission coefficient (C_T) and reflection coefficient (C_R) with structure and environment variables. The structure variables are relative draft (s/h), porosity (p), and relative length of the chamber (L_c/h). The environment variables are relative depth (kh) and wave steepness (H_I/L).

Table 1 Structure variables

Structure Variables					
Variables	Symbol	Prototype		Model	
Draft of the skirt	s_1	3.00	m	25.00	cm
	s_2	2.00	m	16.70	cm
Chamber width	L_{c1}	7.20	m	60.00	cm
	L_{c2}	3.60	m	30.00	cm
Porosity	p_1	50	%	50	%
	p_2	30	%	30	%

Table 2 Environment variables

Environment Variables					
Variables	Symbol	Prototype		Model	
Water depth	H	9.60	m	80.00	cm
		8.40	m	70.00	cm
		7.20	m	60.00	cm
Incident wave height	H_I	1.20	m	10.00	cm
		1.80	m	20.00	cm
		3.60	m	30.00	cm
		4.20	m	35.00	cm
Wave period	T	3.46	s	1.00	s
		6.93	s	2.00	s
		10.39	s	3.00	s
		13.86	s	4.00	s
		17.32	s	5.00	s

3. METHODS

3.1 Models

The Multi-Chamber Skirt Breakwater (MCSB) configuration can be seen in Fig. 1 and Fig. 2, consisting of piles at the lower part and skirts with multi-chambers on the upper part. The skirt has porosity attached to the upper part of the pile, with the part of the skirt is submerged under the water level.

3.2 Laboratory Capacity and Wave Gauges Calibration

The ranges of wave heights and periods that can be generated should be investigated by operating the wave generator at various settings. The wave flume measures 40 m long, 1.5 m deep, and 1.2 m wide. The wave flume can generate wave heights up to 35 cm and wave periods up to 7 seconds.

Four wave gauges are used and calibrated. They are calibrated using the comparison of the wave heights measured manually at the wave flume with data recordings from the wave gauges. Table 3 shows the value of coefficients of calibration for various water depths.

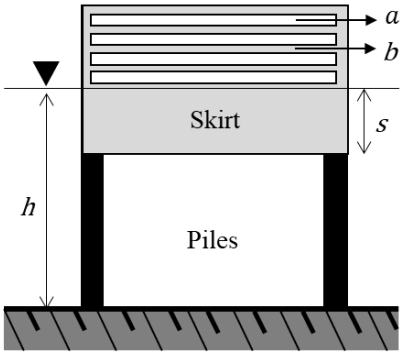

(a) Front view of MCSB

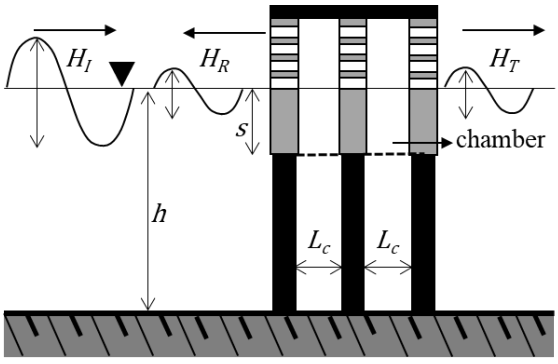

(b) Side view of MCSB.

Fig.1 Definition sketch of MCSB

where

h = water depth
s = draft of the skirt
H_I = incident wave height
H_T = transmitted wave height
H_R = reflected wave height
a = perforated part of the skirt
b = solid part of the skirt
p = $\frac{a}{(a+b)} \times 100\%$ = porosity
L_c = chamber width

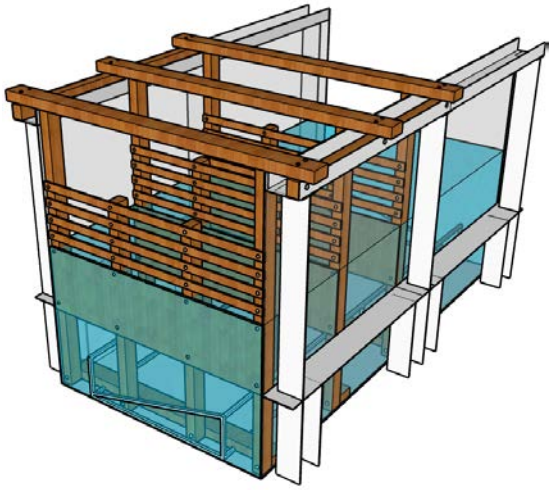

Fig.2 Perspective view of MCSB

Table 3 Value of coefficients of calibration

Water depth (h) [cm]	Coefficient calibration			
	WG1	WG2	WG3	WG4
60	0.024	0.023	0.027	0.023
70	0.033	0.033	0.036	0.034
80	0.041	0.040	0.044	0.039

3.3 Wave Flume Setup

The MCSB model, wave absorber, wave gauges, wavemaker are prepared in the wave flume in the proper position, as seen in Fig. 3.

The wave gauges position is arranged according to the method of Goda and Suzuki (1976) [10], which is formulated in Eq. (5).

$$0.05 < \Delta\ell/L < 0.45 \quad (5)$$

where

$\Delta\ell$ = the distance between two wave gauges (m)
L = wavelength (m)

The closest wave gauge to the model should be placed at a distance of $0.2L$ from the model.

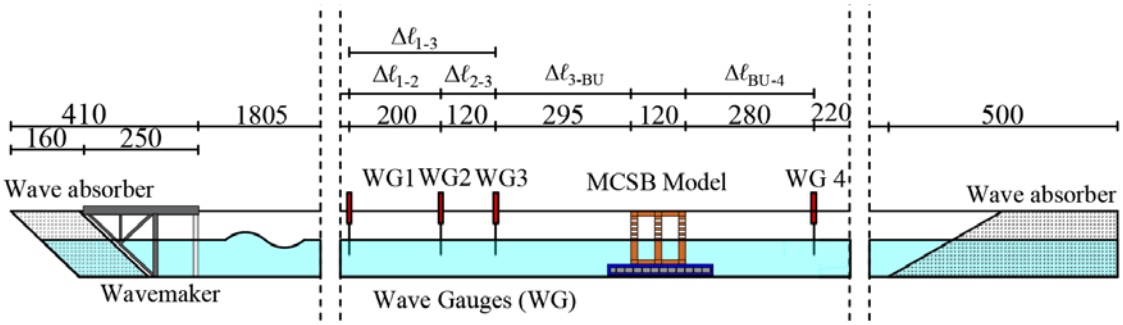

(dimension are in cm)

Fig.3 Waveflume setup

4. EXPERIMENTS

The scenarios of the experiments can be seen in Table 4. There are 480 scenarios. The recorded data for each scenario is 3 minutes minimum.

Table 4 Scenarios of the experiment

Variables	Symbol	Model		Number of Scenarios
Draft of the Skirt	s_1	25.00	cm	2
	s_2	16.70	cm	
Chamber width	L_{c1}	60.00	cm	2
	L_{c2}	30.00	cm	
Porosity	p_1	30	%	2
	p_2	50	%	
Water depth	h	80.00	cm	3
		70.00	cm	
		60.00	cm	
Incident Wave height	H_I	10.00	cm	4
		20.00	cm	
		30.00	cm	
		35.00	cm	
Wave Periode	T	1.00	s	5
		2.00	s	
		3.00	s	
		4.00	s	
		5.00	s	

5. DATA ANALYSIS

The data recorded by the wave gauges 1, 2, 3 (incident wave), and wave gauge 4 (transmitted wave) are used to calculate the transmission coefficient. The reflected coefficient is calculated using the wave gauges 1-2, 2-3, and 1-3.

The data recorded from the wave gauges are processed using zero-mean processes. The selection of time interval data to be analyzed is determined, i.e., the time-lapse in the wave record that has not been affected by the reflected waves.

The result of the analysis is a nondimensional graph of C_T and C_R versus structure and environmental variables.

5.1 Wave Transmission Analysis

Transmission coefficients (C_T) are defined as the ratio between the transmitted and incident wave heights. The incident waves are calculated from the zero up crossing process of water level elevation recorded by the wave gauges in front of the model. The transmitted waves are the zero-up crossing of water level elevation from the model's wave gauges.

The transmission coefficients, C_T, *are* defined in Eq. (6).

$$C_T = \frac{\bar{H}_T}{\bar{H}_I} \tag{6}$$

where

C_T = transmission coefficient
$\bar{H}_I$ = average of incident wave height (m)
$\bar{H}_T$ = average of transmitted wave height (m)

5.2 Wave Reflection Analysis

The wave reflection analysis is calculated based on a technique to resolve the incident and reflected waves from the record of composite waves. This technique is introduced by Goda and Suzuki (1976) [12].

Reflection Coefficient (C_R) analysis is obtained from comparing the incident wave energy and the reflection wave energy, as shown in Eq. (7).

$$C_R = \sqrt{\frac{E_R}{E_I}} \tag{7}$$

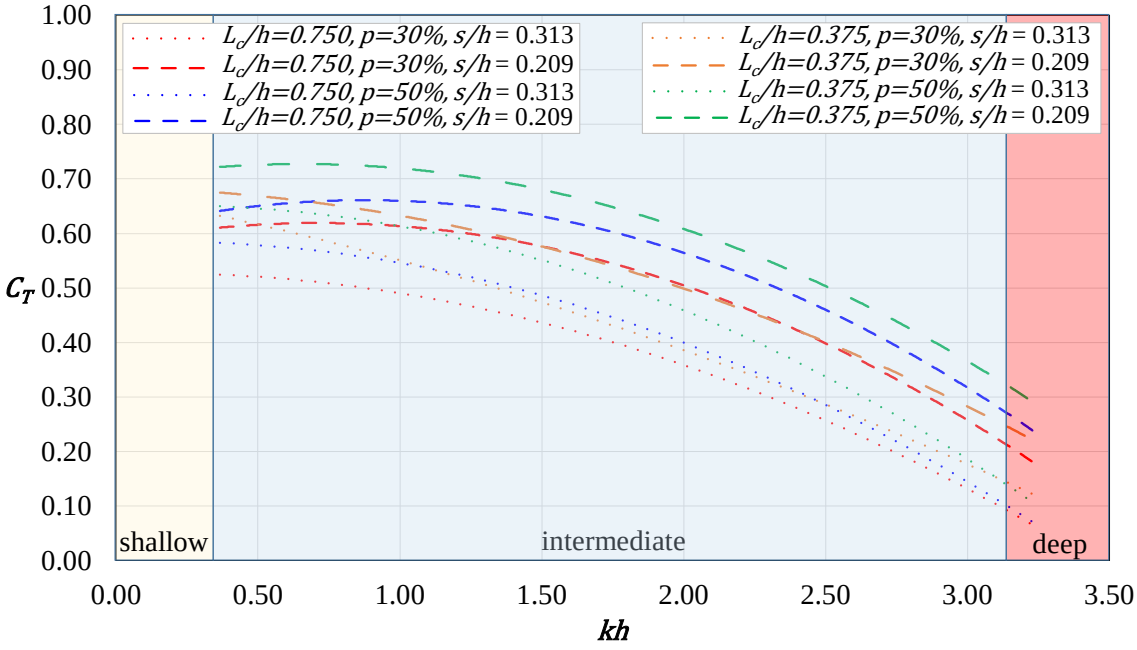

Fig. 4 Graph of C_T vs. kh as a function of s/h, p, and L_c/h

where
C_R = reflection coefficient
E_I = incident wave energy
E_R = reflected wave energy.

The wave energy of incident and reflected waves are obtained from Eqs. (8) and (9).

$$E_I = \int_{i=0}^{i=N} S_I(\omega)d\omega \quad (8)$$

$$E_R = \int_{i=0}^{i=N} S_R(\omega)d\omega \quad (9)$$

where
$S_I(\omega)$ = incident wave spectrum (m^2s)
$S_R(\omega)$ = reflected wave spectrum (m^2s)
ω = wave angular frequency (rad/s)

The incident and reflected wave spectrum are obtained from the component of the amplitude spectrum calculation, according to Eqs. (10) and (11).

$$S_I(\omega)=\frac{\frac{1}{2}{a_{I_i}}^2}{\Delta\omega} \quad (10)$$

$$S_R(\omega)=\frac{\frac{1}{2}{a_{R_i}}^2}{\Delta\omega} \quad (11)$$

a_{I_i} and a_{R_i} are the amplitude of the spectrum components of the incident and reflected waves obtained from Goda and Suzuki (1976) [11].
The amplitude spectrum is obtained from the following Eq. (12) and Eq. (13).

$$a_{I_i} = \frac{1}{2|\sin k_i \Delta\ell|}\left[\left(a_{2_i} - b_{1_i}\cos k_i\,\Delta\ell - b_{1_i}\sin k_i\,\Delta\ell\right)^2 + \left(b_{2_i} - b_{1_i}\cos k_i\Delta\ell + a_{1_i}\sin k_i\Delta\ell\right)^2\right]^{1/2} \quad (12)$$

$$a_{R_i} = \frac{1}{2|\sin k_i \Delta\ell|}\left[\left(a_{2_i} - b_{1_i}\cos k_i\,\Delta\ell + b_{1_i}\sin k_i\,\Delta\ell\right)^2 + \left(b_{2_i} - b_{1_i}\cos k_i\Delta\ell - b_{1_i}\sin k_i\Delta\ell\right)^2\right]^{1/2} \quad (13)$$

where
a_{1i}, b_{1i} = Fourier coefficient of WG1 data
a_{2i}, b_{2i} = Fourier coefficient of WG2 data
k = wave number (m^{-1})
L = wavelength (m)
$\Delta\ell$ = distance of WG1 and WG2 (m)

6. RESULTS AND DISCUSSIONS

The results of the physical modeling are described by using nondimensional plots in Figures 4-7. The figures show the relationship between C_T and C_R values with the values of environment variables kh and H_I/L. The optimum performance of MCSB is described in Fig.8.

The plots are varied according to the structure variables s/h, L_c/h, and p in the intermediate depth water dan deepwater regions.

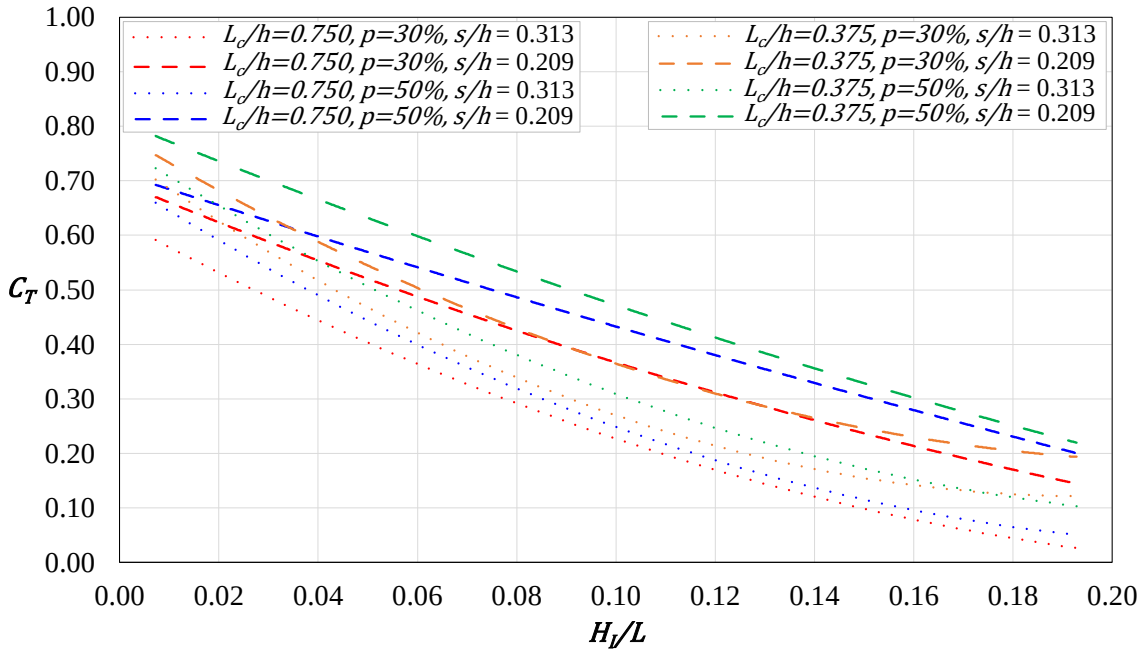

Fig. 5. Graph of C_T vs. H_I/L as a function of s/h, p, and L_c/h

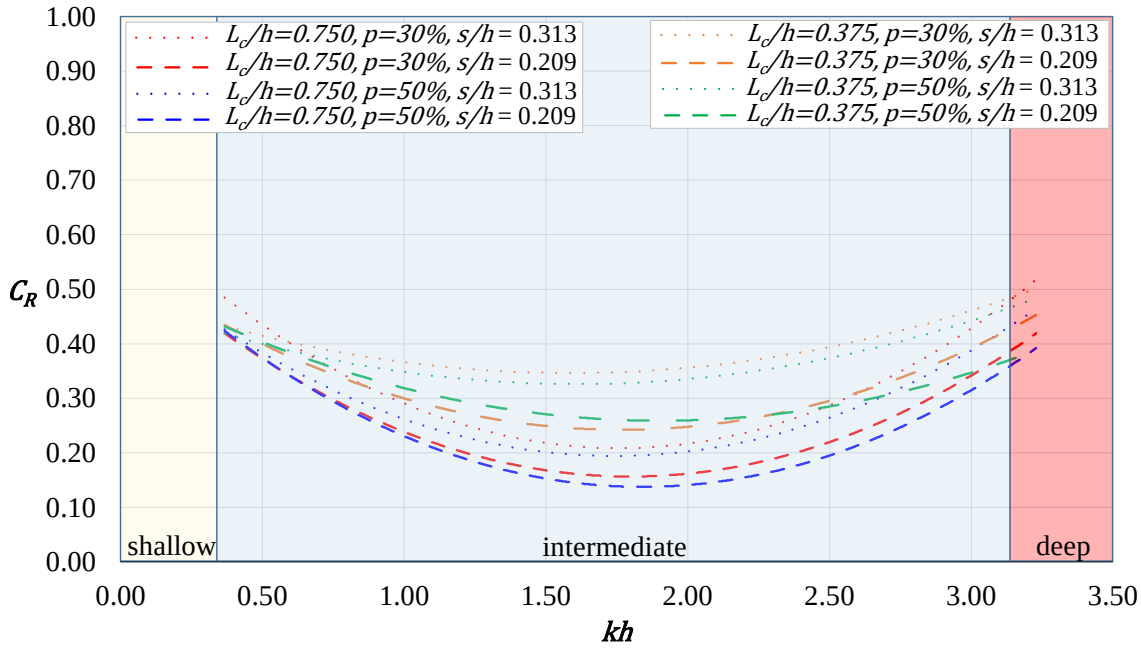

Fig. 6. Graph of C_R vs H_I/L as a function of s/h, p, and L_c/h

6.1 Transmission Coefficient, C_T

Figure 4 shows the relation between C_T and kh (environment variable) as a function of s/h, p, and L_c/h (structure variables). As indicated by the figure, C_T decreases as kh increases, or the MCSB is more effective in deep water ($0.06<C_T<0.29$) compared to intermediate depth water ($0.10<C_T<0.70$).

The relation of structure variables (s/h, p, and L_c/h) with C_T in Fig. 4 concludes that C_T increases as s/h decreases, p increases, and L_c/h decreases.

Figure 5 shows the relation between C_T and H_I/L (environment variable) as a function of s/h, p, and L_c/h (structure variables). As indicated by the figure, C_T decreases following the increase of H_I/L.

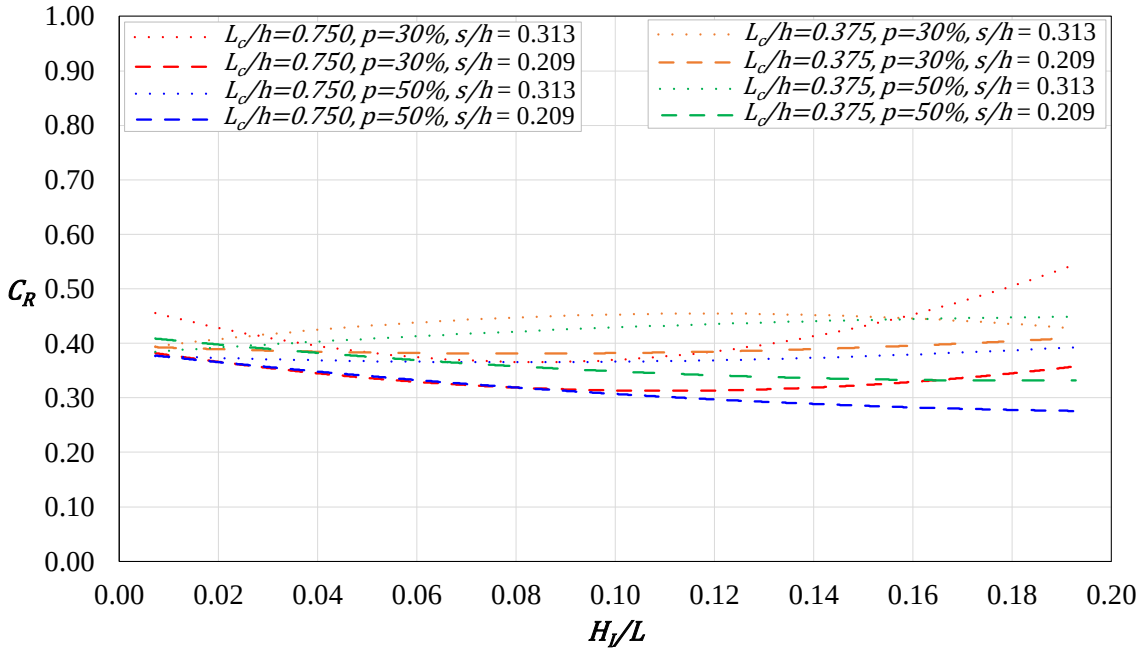

Fig. 7. Graph of C_R *vs* H_I/L as a function of s/h, p, and L_c/h

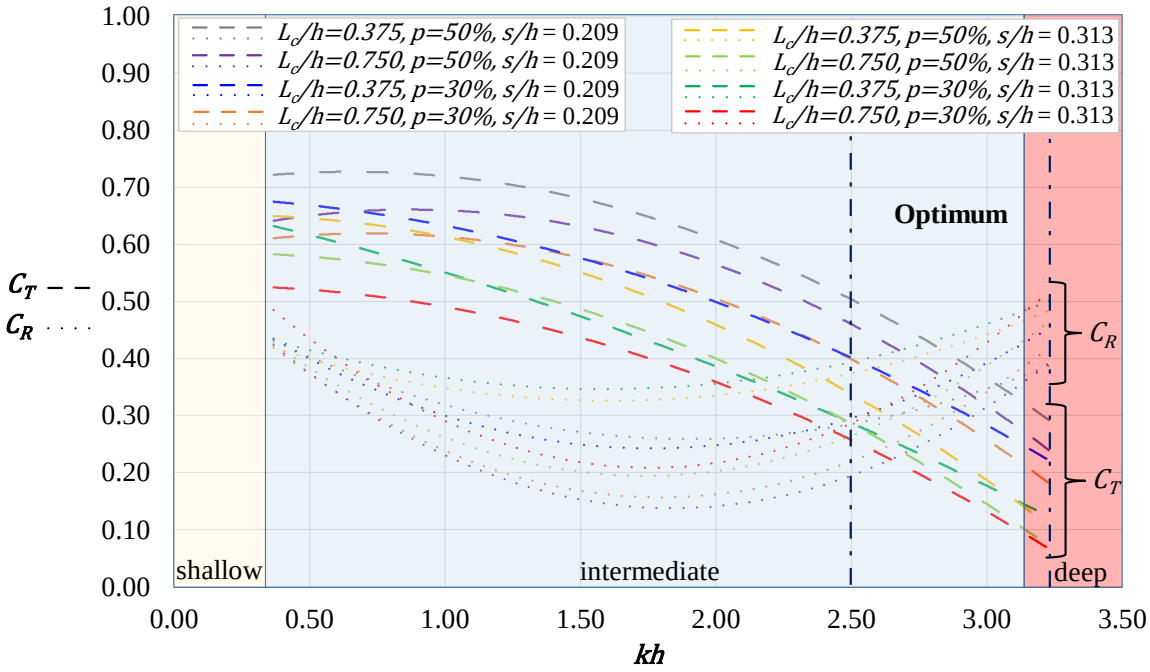

Fig. 8. Graph of C_R and C_T *vs* kh as a function of s/h, p, and L_c/h

The relation of structure variables (s/h, p, and L_c/h) with C_T in Fig. 5 concludes that C_T increases as s/h decreases, p increases, and L_c/h decreases.

6.2 Reflection Coefficient, C_R

Figure 6 shows the relation between C_R and kh (environment variable) as a function of s/h, p, and L_c/h (structure variables). The values of C_R in the Deepwater is $0.39<C_R<0.52$. They are higher than those in the intermediate water depth, which are $0.14<C_R<0.49$.

The relation of structure variables (s/h, p, *and* L_c/h) with C_R in Fig. 6 concludes that C_R is increasing if s/h increases, p decrease, and L_c/h decrease.

Figure 7 shows the relation between C_R and H_I/L (environment variable) as a function of s/h, p, and

L_c/h (structure variables). The C_R does not change significantly to H_I/L, with the value of C_R is $0.28<C_R<0.54$.

6.3 Transmission Coefficients, C_T and Reflection Coefficients, C_R

Figure 8 shows both C_T and C_R as a function of structural variables (s/h, p, and L_c/h), described as the optimum performance of MCSB. The optimum performance occurred if the wave transmission and wave reflection are small or the value of C_T and C_R are not more than 0.5. The optimum condition of MCSB occurs in the range of $2.50<kh<3.10$, which shows the value of C_T and C_R is below 0.5.

These C_T and C_R values explain the physical conditions of the transmission waves behind the MCSB are small. The reflection waves in front of the MCSB are also small (the effectiveness of MCSB is more than 50%).

The most effective MCBS structure configuration based on C_T value is a structure with $L_c/h=0.75$, $p=30\%$ and $s/h=0.313$. While the most effective MCSB structure based on C_R value is a structure with $L_c/h=0.75$, $p=50\%$ and $s/h=0.209$.

7. CONCLUSIONS

The MCSB has an optimum performance if C_T and C_R are small, or the values are less than 0.5. The C_T and C_R are relatively low (less than 0.52) in the deepwater region. The effectiveness of MCSB in deep water occurs because of the skirt porosity, which results in a decrease of C_R. It is concluded that the MCSB is useful in deep water.

The C_R is small in the intermediate depth water. The value of C_R is less than 0.52 in the range of depth $2.50<kh<3.10$. The C_T is high in the interval of $0.314<kh<2.50$ ($C_T>0.5$) but small in $kh>2.50$. It is concluded that the MCSB is still effective in the intermediate depth water condition if $kh>2.50$.

The draft, porosity, and chamber gap width of the MCSB significantly influence C_T and C_R. The selection of skirt draft, porosity, and chamber width dimensions need to be considered. The higher s and p, the lower C_T while at the same time, the C_R increases. The higher chamber width (L_c), the higher C_T. However, the value of C_R decreases.

8. REFERENCES

[1] Takahashi S., Breakwater Design (Tsinker G.P, Handbook of Port and Harbor Engineering), Chapman and Hall: the United States of America, 1997.

[2] Dalrymple R. A. and Dean R.G., Water Wave Mechanics for Engineers and Scientists, World Scientific Publishing: Singapore, 1991.

[3] Suh K.D., Shin, S., Cox, D.T. Hydrodynamic Characteristics of Curtain-Wall-Pile Breakwaters. XXXI IAHR CONGRESS, Seoul, Korea, 2005.

[4] Koraim A.S., Hydrodynamic Characteristics of Slotted Breakwaters Under Regular Waves, Journal of Marine Science Technology, Vol. 16, 2011, pp. 331-342.

[5] Wurjanto A., Ajiwibowo H. and Zamzani R., 2D Physical Model to Measure The Effectiveness Perforated Skirt Breakwater on The Longwave Category. Theory and application of Civil Engineering Jurnal, Vol.17, No.3, 2010.

[6] Laju K., Sundar V., Sundaravadivelu R., Studies on Pile Supported Skirt Breakwater, The Journal of Ocean Technology, Vol. 2(1), 2007, pp. 1-22.

[7] Suh K.D., Jung H.Y., Pyun C.K., Wave Reflection, and Transmission by Curtain Wall Pile Breakwaters Using Circular Piles, Ocean Engineering, Vol. 34, 2007, pp. 2100–2106.

[8] Ajiwibowo H. Three-dimensional Physical Modeling on Perforated Skirt Breakwater. International Journal of Engineering and Technology (IJET), Vol.9, No. 6, 2017, pp., 4069-4080.

[9] Ajiwibowo H. 2-D Physical Modeling for Measuring The Effectiveness of Single Curtain Pile Foundation Breakwater in Intermediate Water Depth, International Journal of GEOMATE, Vol.14, Issue 43, 2018, pp. 160-166.

[10] Ajiwibowo H. 2-D Physical Modeling to Measure The Effectiveness of Perforated Skirt Breakwater for Short Period Waves, ITB J.Eng.Sci, Vol.43, No.1, 2011, pp. 57-78.

[11] Hughes S.A., Physical Models and Laboratory Techniques in Coastal Engineering, World Scientific Publishing: Singapore, 1993.

[12] Goda Y. and Suzuki T., Estimation of Incident and Reflected Waves in Random Wave Experiment, Coastal Engineering Proceedings, Vol. 1, No.15, 1976, pp. 47.